# Orientational regularities in two-dimensional quasidipole system with degenerate ground states

V. M. Rozenbaum,[1,2,*] A. N. Morozov,[2] and S. H. Lin[1]

[1]*Institute of Atomic and Molecular Sciences, Academia Sinica, P.O. Box 23-166, Taipei, Taiwan, Republic of China*
[2]*Institute of Surface Chemistry, National Academy of Sciences of Ukraine, Generala Naumova str. 17, Kiev, 03164, Ukraine*

A two-dimensional quasidipole system with discrete moment orientations and a degenerate ground state (at the temperature $T=0$) is modeled by a Hamiltonian for a pair of Ising subsystems ($\sigma$ and $s$) coupled by a so-called fluctuation interaction vanishing at $T=0$. A system of this kind is proved to reduce to a special case of the anisotropic spin-3/2 Ising model. A phase diagram in the coordinates $T/J_1$ and $J_2/J_1$ is constructed ($J_1$ is the constant of the $\sigma$-$\sigma$ and $s$-$s$ interactions, $J_2$ is the constant of the fluctuation $\sigma$-$s$ interactions, and $T$ is the absolute temperature in energy units) based on the analytical solution for the Bethe lattice with the coordination number 4 and on the Monte Carlo simulation for a square lattice. In addition to ordinary phases, a high-temperature disordered phase I ($\langle \sigma \rangle = \langle s \rangle = 0$) and a low-temperature ordered phase II ($\langle \sigma \rangle$ and $\langle s \rangle \neq 0$), an intermediate-temperature correlated phase III ($\langle \sigma s \rangle \neq 0$ at $\langle \sigma \rangle = \langle s \rangle = 0$) is also possible for the system concerned at values $J_2$ close to $J_1$. For strong fluctuation interaction $J_1 = J_2$, an exact solution of the statistical problem on a square lattice is obtained. For a quasidipole system, phase III corresponds to an orientational ordering with spontaneous anisotropy but without polarization and is observable in the monolayers of adsorbed molecules.

## I. INTRODUCTION

Among various systems with complex periodic orientations of magnetic or electric moments, those with a continuously degenerate ground state occupy a special place. Such a degeneracy usually corresponds to certain rotations of the moments in antiferromagnetic sublattices, and can be removed by thermodynamic fluctuations, which occasionally leads to interesting physical effects (so-called "ordering due to disorder").[1,2] Within this class, the two-dimensional (2D) dipole model[3–5] is particularly promising, since it is applicable to phase transitions in real systems consisting not only of 2D antiferromagnets with dipole interactions but of adsorbed molecules as well.[6,7] The latter systems are also characterized by adsorption potentials whose azimuthal symmetry enables the development of models with discrete orientations of the dipole moments. Such models are promising both in an applied treatment of concrete adsorbates and in fundamental studies of systems with a degenerate ground state. This significant aspect deserves detailed consideration.

A treatment of lattice systems with discrete moment orientations can be reduced to models in which each lattice site is characterized by several spin variables. Such models (exemplified by the well-known Ashkin-Teller model[8–10]) generalize the Ising model and in some cases admit exact solutions which are of paramount importance in the phase transition theory. For the degenerate ground state, the Hamiltonian and the corresponding solutions have such a structure which describes an unusual orientational behavior of the system within a certain region of the values of spin interaction constants. The properties of such systems are detailed in the present paper.

In Sec. II, we start from a general form of the quasidipole Hamiltonian of a 2D system of moments with four possible orientations on a square lattice and derive the corresponding Hamiltonian in terms of spin variables $\sigma$ and $s$ which covers not only ordinary $\sigma$-$\sigma$ and $s$-$s$ interactions (with the interaction constant $J_1$) but also the so-called fluctuation $\sigma$-$s$ interactions ($J_2$), giving no contribution to the degenerate ground state. This degeneracy originates from the fact that the fluctuation interactions along horizontal and vertical lattice bonds give canceling contributions of opposite sign in the ground state. As a consequence, the model in question is essentially anisotropic. Evidently, a system with a pair of spins, $\sigma = \pm 1$ and $s = \pm 1$, should be equivalent to a spin-3/2 Ising model whose isotropic versions have been under vigorous investigation (see, for instance, Refs. 11 and 12 and the references therein). That is why here we also give an alternative representation of the Hamiltonian derived in terms of the anisotropic spin-3/2 Ising model.

An exact solution for the above-formulated model has been unknown for a square lattice with arbitrary values of the constants $J_1$ and $J_2$; nor can the self-consistent-field approximation describe the fluctuation interactions. Thus, it is reasonable to invoke the prototype of this model on the Bethe lattice (according to the approach of Baxter,[10] the solutions obtained for the Bethe lattice can be regarded as exact ones). In Sec. III, a phase diagram is constructed in the coordinates $T/J_1$ and $J_2/J_1$ ($T$ the absolute temperature in energy units) which includes, in addition to the ordinary phases, *viz.* the high-temperature disordered phase I ($\langle \sigma \rangle = \langle s \rangle = 0$) and low-temperature ordered phase II ($\langle \sigma \rangle$ and $\langle s \rangle \neq 0$), an intermediate-temperature correlated phase III ($\langle \sigma s \rangle \neq 0$ at $\langle \sigma \rangle = \langle s \rangle = 0$). A phase of this kind resembles that arising in the well-known Ashkin-Teller model,[8–10] but, in our treatment, i.e., in terms of the quasidipole model, it corresponds to an orientational ordering with spontaneous anisotropy but without polarization.

In the case $J_2 = J_1$, the low-temperature phase II can exist only in the ground state, and the system is characterized by a single transition between phases I and III at nonzero temperatures. It turns out that this important special case admits

an exact solution of the statistical problem also for a square lattice (see Sec. IV). The partition function under study enables states for one spin subsystem to be summed up in an explicit form. Then the sum over the states of the second spin subsystem is formally expressible in terms of the partition function of the 2D Ising model with an unusual interaction parameter which is thermodynamically averaged over the spins of the first subsystem. To extend the phase diagram on a square lattice to the region of intermediate values of the fluctuation interaction constant $(0 \leq J_2 \leq J_1)$, the Monte Carlo simulation is invoked. In Sec. V we consider an orientational phase transition in the monolayer CO/NaCl(100) which represents the I-II transition, and also discuss the possibility for phase III to be detected experimentally.

The paper includes an appendix of independent interest. It presents a straightforward analytical approach to the expression for the free energy and also to the equations of state for an arbitary-spin system in an external field on the anisotropic Bethe lattice. The relations derived are extremely compact and easy to apply in further calculations. The efficiency of the technique developed is demonstrated well by a brief and easy derivation of the expression for the free energy in the anisotropic Ising model on the Bethe lattice. (This formula is normally obtained by a tedious integration of the equations of state over the external field[10]). The same general relations are also involved in Sec. III to analyze the states of a system with fluctuation interactions.

## II. ISING-LIKE HAMILTONIAN WITH FLUCTUATION INTERACTION

Consider the general form of the dipole Hamiltonian

$$H_{Dip} = \sum_{mn} [D_1(\mathbf{e}_{mn} \cdot \mathbf{e}_{m+1,n} + \mathbf{e}_{mn} \cdot \mathbf{e}_{m,n+1})$$

$$+ D_2(e^x_{mn} e^x_{m+1,n} + e^y_{mn} e^y_{m,n+1})] \quad (1)$$

($\mathbf{e}_{mn}$ denotes the unit vectors, and $e^x_{mn}$ and $e^y_{mn}$ are their projections onto the square lattice axes) in which the parameters $D_1$ and $D_2$ can differ from the standard values $D_1 = \mu^2/a^3$, $D_2 = -3\mu^2/a^3$ ($\mu$ is the dipole moment, and $a$ is the lattice constant), provided the systems concerned have surface-quasinormal[13] or surface-parallel[14] orientations of nonpolar molecules. In this case, the parameters $D_1$ and $D_2$ are governed by the constants of actual interactions (quadrupole, van der Waals, etc.) or by the parameters of the Lennard-Jones potential. At $0 < D_1 < -D_2$, the ground state of the system with $N$ lattice sites, $H_0 = -N|D_2|$, is degenerate in the parameter $D_1$. The degeneracy is, however, removed with rising temperature, which gives rise to collinear orientations of dipole moments along any of the square lattice axes[5] and results in the stabilization of the long-range orientational order.[15] If the systems of adsorbed molecules are characterized by the adsorption potential of the symmetry $C_4$ which strongly depends upon the azimuthal angle, only four discrete orientations (along the axes of the square lattice) may prove allowed for the vectors $\mathbf{e}_{mn}$ [as, for instance, in the $2 \times 1$ monolayer of CO molecules adsorbed on the
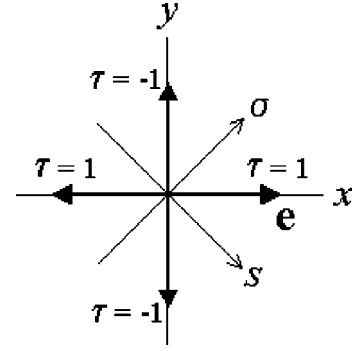


FIG. 1. The correspondence between four orientations of the vectors $\mathbf{e}_{mn}$ and four pairs of values of spin variables, $\sigma_{mn} = \pm 1$ and $s_{mn} = \pm 1$ (or $\tau_{mn} = \sigma_{mn} s_{mn}$).

NaCl(100) surface[16]]. With the orientations $\mathbf{e}_{mn}$ specified by the spin variables $\sigma_{mn}$ and $s_{mn}$ (see Fig. 1):

$$\mathbf{e}_{mn} = \frac{1}{2}[(-1)^n(\sigma_{mn} + s_{mn}), (-1)^m(\sigma_{mn} - s_{mn}), 0], \quad (2)$$

Hamiltonian (1) reduces to the following form:

$$H = \sum_{mn} [-J_1(\sigma_{mn}\sigma_{m+1,n} + s_{mn}s_{m+1,n}$$

$$+ \sigma_{mn}\sigma_{m,n+1} + s_{mn}s_{m,n+1})$$

$$- J_2(\sigma_{mn}s_{m+1,n} + s_{mn}\sigma_{m+1,n} - \sigma_{mn}s_{m,n+1}$$

$$- s_{mn}\sigma_{m,n+1})], \quad (3)$$

with $J_1 = -D_2/4$ and $J_2 = -D_2/4 - D_1/2$. At $0 \leq J_2 \leq J_1$, the ground state of this Hamiltonian, $H_0 = -4NJ_1$, is independent of the interaction constant $J_2$ between $\sigma$ and $s$ spins. The ground state degeneracy also occurs at arbitrary $J_1$ to $J_2$ ratios. Figure 2 demonstrates the phase diagram of the ground states. Clearly, the spin variables can be relabeled so that each phase region is describable by Hamiltonian (3) with the substitution $J_1 \leftrightarrow J_2$ and/or the change of $J_1$ and $J_2$ signs. As a result, all the phase regions have the same statistical properties and we can limit the consideration to the region $0 \leq J_2 \leq J_1$ without loss of generality.

It is conceptually impossible to analyze the states of such systems within the framework of the self-consistent-field approximation which neglects the interaction of thermodynamic fluctuations, since the sum of products of average spins $\langle\sigma\rangle\langle s\rangle$ goes to zero and the dependence on $J_2$ vanishes. We therefore use the term *fluctuation interactions* for the interactions between the spin subsystems $\sigma$ and $s$ described by Hamiltonian (3). Discussing the models with interacting Ising subsystems, one cannot but mention the well-known isotropic model of Ashkin and Teller,[8]

$$H_{AT} = \sum_{mn} [-J_1(\sigma_{mn}\sigma_{m+1,n} + s_{mn}s_{m+1,n} + \sigma_{mn}\sigma_{m,n+1}$$

$$+ s_{mn}s_{m,n+1}) - J_4(\sigma_{mn}s_{mn}s_{m+1,n}\sigma_{m+1,n}$$

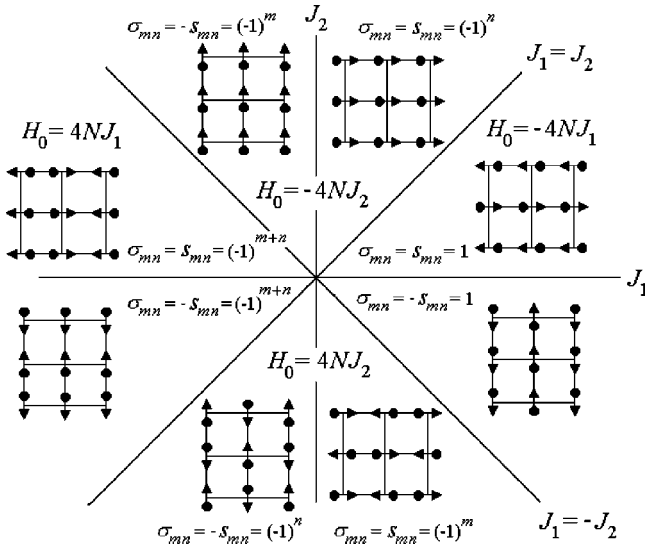$$+ \sigma_{mn}s_{mn}\sigma_{m,n+1}s_{m,n+1})], \quad (4)$$

FIG. 2. The phase diagram for the ground states of two Ising subsystems on a square lattice, with fluctuation interaction between them [see Eq. (3)]. Four phase regions are separated by the straight lines $J_1 = \pm J_2$. Each phase is characterized by two degenerate states corresponding to the horizontal and vertical orientations of the unit vectors $\mathbf{e}_{mn}$ represented by the arrows and specified by Eq. (2) (also see Fig. 1).

with its phase diagram basically reproducible even in the self-consistent-field approximation.[9,10] It is noteworthy that Hamiltonian (3) with the additional term $J_4 < 0$ from Eq. (4) accounts for the orientational properties of the system CO/NaCl(100).[13]

It should be noted that a system with a pair of spins, $\sigma = \pm 1$ and $s = \pm 1$, positioned at each lattice site is essentially equivalent to a spin-3/2 Ising model. So far, only isotropic particular cases of this model have been attracting theoretical interest. In the framework of this model, the Hamiltonian covering various interactions of spins $S = \pm 1/2, \pm 3/2$ between the neighboring sites $i$ and $j$ of an arbitrary lattice is normally written in the form[11,12]

$$H = -\frac{1}{2}\sum_{i \neq j}\left[ JS_i S_j + KS_i^2 S_j^2 + LS_i^3 S_j^3 + \frac{M}{2}(S_i S_j^3 + S_i^3 S_j)\right]$$
$$-\Delta \sum_i S_i^2. \tag{5}$$

The simplest relation between the spins $S_i$ and $\sigma_i$, $s_i$ appears as

$$S_i = \sigma_i + \frac{1}{2}s_i. \tag{6}$$

Substituting Eq. (6) into Eq. (5) affords the Hamiltonian in terms of the variables $\sigma$ and $s$:

$$H = -\frac{1}{2}\sum_{i \neq j}\left[ J_1\sigma_i\sigma_j + J_1's_i s_j + J_2(\sigma_i s_j + s_i\sigma_j) + J_4\sigma_i s_i\sigma_j s_j \right.$$
$$\left. + \frac{25}{16}J_4 + \frac{5}{4}J_4(\sigma_i s_i + s_j\sigma_j)\right] - \Delta\sum_i\left(\frac{5}{4} + \sigma_i s_i\right), \tag{7}$$

into which the new interaction constants enter:

$$\begin{pmatrix} J_1 \\ J_1' \\ J_2 \end{pmatrix} = \begin{pmatrix} 1 & 49/16 & 7/4 \\ 1/4 & 169/64 & 13/16 \\ 1/2 & 91/32 & 5/4 \end{pmatrix}\begin{pmatrix} J \\ L \\ M \end{pmatrix}, \quad J_4 = K. \tag{8}$$

Comparing Hamiltonians (4) and (7), one can see that a spin-3/2 Ising model is equivalent to the Ashkin-Teller model with an additional term proportional to the interaction constant $J_2$ (one-site interactions $\sigma_i s_i$ can be nullified by the appropriate choice of the constant $\Delta$). It follows thereto that at $J_2 = 0$, a spin-3/2 Ising model is also reducible to the eight-vertex model (a relevant deduction was reported in Refs. 11 and 12, the latter involving a less general condition than $J_2 = 0$ used here).

An anisotropic spin-3/2 Ising model can be formulated as a model described by Hamiltonian (7), with the interaction constants differing for differently oriented ($ij$) bonds. For a square lattice, Hamiltonians (3) and (7) correlate with the proviso that $J_1 = J_1'$, $J_4 = \Delta = 0$, and the constant $J_2$ alternates in sign along the horizontal and vertical bonds. At $J_4 = -\Delta/5 \neq 0$, a generalized Ashkin-Teller model results, which includes fluctuation interactions (the full analysis of its properties will be presented elsewhere). Labeling interaction constants along the horizontal and vertical bonds by the indices $x$ and $y$ in Hamiltonian (7), we arrive at the following relations:

$$M_{x,y} = -\frac{4}{5}J_{x,y} - \frac{9}{20}L_{x,y}, \quad J_x + J_y = \frac{73}{16}(L_x + L_y), \tag{9}$$

which establish a univocal correspondence between the anisotropic spin-3/2 Ising model and the generalized Ashkin-Teller model with fluctuation interactions.

### III. PHASE TRANSITIONS ON THE BETHE LATTICE

The partition function for Hamiltonian (3) on a Cayley tree with the coordination number 4 and $N$ shells ($N = 0$ for the tree leaves) can be represented as

$$Z(N) = \sum_{i=1}^4 x_i^2(N)y_i^2(N), \tag{10}$$

where the values $x_i(N)$ and $y_i(N)$ are determined for a certain deeply lying node of the tree by a system of recurrent equations:

$$x_i(N) = \sum_{j=1}^4 \Lambda_{ij}^{(x)} x_j(N-1)y_j^2(N-1),$$

$$y_i(N) = \sum_{j=1}^4 \Lambda_{ij}^{(y)} y_j(N-1)x_j^2(N-1). \tag{11}$$

Here the indices $i$, $j = 1$, 2, 3, 4 respectively refer to the following coupled values of the spin variables $\sigma$ and $s$: $+1$, $+1$; $-1$, $-1$; $+1$, $-1$; $-1$, $+1$. The matrices $\Lambda^{(x)}$ and $\Lambda^{(y)}$ of the dimensionality $4 \times 4$ are expressible in block form:

$$\Lambda^{(x)}=\begin{pmatrix} A & C \\ C & B \end{pmatrix},\Lambda^{(y)}=\begin{pmatrix} B & C \\ C & A \end{pmatrix},$$

$$A=\begin{pmatrix} e^{2(K_1+K_2)} & e^{-2(K_1+K_2)} \\ e^{-2(K_1+K_2)} & e^{2(K_1+K_2)} \end{pmatrix},$$

$$B=\begin{pmatrix} e^{2(K_1-K_2)} & e^{-2(K_1-K_2)} \\ e^{-2(K_1-K_2)} & e^{2(K_1-K_2)} \end{pmatrix},$$

$$C=\begin{pmatrix} 1 & 1 \\ 1 & 1 \end{pmatrix}, \tag{12}$$

with $K_{1,2}=J_{1,2}/T$ ($T$ is the absolute temperature in energy units).

For an arbitrary spin system on an anisotropic Cayley tree with the coordination number $q$, we derive a general formula for the free energy of the corresponding Bethe lattice (associated with the Cayley tree given at $N\to\infty$)—see the Appendix. At $q=4$, this relation affords the free energy of the system concerned (per site of the Bethe lattice):

$$f_{Bethe}=T\ln Z, \tag{13}$$

where $Z$ is specified by Eq. (10) with the quantities $x_i$ and $y_i$ (already independent of $N$) obeying the system of equations (11). In other words, recurrent equations (11) in the limit $N\to\infty$ determine a stable point $x_i$, $y_i$ which defines, in turn, the free energy (13). The same quantities specify the averages of the spin variables:

$$\langle\sigma\rangle=Z^{-1}\sum_{i=1}^{4}\sigma_i x_i^2 y_i^2, \quad \langle s\rangle=Z^{-1}\sum_{i=1}^{4}s_i x_i^2 y_i^2,$$

$$\langle\sigma s\rangle=Z^{-1}\sum_{i=1}^{4}\sigma_i s_i x_i^2 y_i^2. \tag{14}$$

The eigenvalues of the matrices $\Lambda^{(x)}$ and $\Lambda^{(y)}$,

$$\lambda_1=a_1, \ \lambda_2=b_1, \ \lambda_{3,4}=\frac{1}{2}[a_2+b_2\mp c],$$

$$c=\sqrt{(a_2-b_2)^2+16}, \tag{15}$$

are convenient to manipulate, as they are expressible in terms of the eigenvalues of the matrices $A$ and $B$:

$$a_1=2\sinh 2(K_1+K_2), \quad a_2=2\cosh 2(K_1+K_2),$$

$$b_1=2\sinh 2(K_1-K_2), \quad b_2=2\cosh 2(K_1-K_2). \tag{16}$$

The eigenvectors of the $\Lambda^{(x)}$ and $\Lambda^{(y)}$ are expressible as the block-structured matrices:

$$S^{(x)}=\begin{pmatrix} S_1 & S_3 \\ S_2 & S_4 \end{pmatrix}, \quad S^{(y)}=\begin{pmatrix} S_2 & S_4 \\ S_1 & S_3 \end{pmatrix},$$

$$S_1=\begin{pmatrix} 2^{-1/2} & 0 \\ -2^{-1/2} & 0 \end{pmatrix}, \quad S_2=\begin{pmatrix} 0 & 2^{-1/2} \\ 0 & -2^{-1/2} \end{pmatrix},$$

$$S_{3,4}=\begin{pmatrix} (c\gamma_{3,4})^{-1/2} & (c\gamma_{4,3})^{-1/2} \\ (c\gamma_{3,4})^{-1/2} & (c\gamma_{4,3})^{-1/2} \end{pmatrix}, \tag{17}$$

where

$$\gamma_{3,4}=\frac{1}{4}[c\pm(a_2-b_2)], \quad \gamma_3\gamma_4=1. \tag{18}$$

Then the system of equations (11) in the limit $N\to\infty$ appears as follows:

$$\sum_{i=1}^{4}(1-\lambda_k y_i^2)S_{ik}^{(x)}x_i=0, \quad \sum_{i=1}^{4}(1-\lambda_k x_i^2)S_{ik}^{(y)}y_i=0,$$

$$k=1,2,3,4. \tag{19}$$

Introducing the ratios of the variables $x_i$ and $y_i$,

$$\xi_{ij}=\frac{x_i}{x_j}, \quad \eta_{ij}=\frac{y_i}{y_j}. \tag{20}$$

we rewrite Eqs. (19) in an explicit form:

$$x_1^2=\frac{1-\eta_{12}}{\lambda_2(\xi_{21}^2-\eta_{12})}=\frac{1-\eta_{34}}{\lambda_1(\xi_{43}^2-\eta_{34})\xi_{31}^2}$$

$$=\frac{1+\eta_{34}-\gamma_3(1+\eta_{12})\eta_{24}}{\lambda_3[(\xi_{43}^2+\eta_{34})\xi_{31}^2-\gamma_3(\xi_{21}^2+\eta_{12})\eta_{24}]}$$

$$=\frac{1+\eta_{34}+\gamma_4(1+\eta_{12})\eta_{24}}{\lambda_4[(\xi_{43}^2+\eta_{34})\xi_{31}^2+\gamma_4(\xi_{21}^2+\eta_{12})\eta_{24}]},$$

$$y_4^2=\frac{1-\xi_{43}}{\lambda_2(\eta_{34}^2-\xi_{43})}=\frac{1-\xi_{21}}{\lambda_1(\eta_{12}^2-\xi_{21})\eta_{24}^2}$$

$$=\frac{1+\xi_{21}-\gamma_3(1+\xi_{43})\xi_{31}}{\lambda_3[(\eta_{12}^2+\xi_{21})\eta_{21}^2-\gamma_3(\eta_{34}^2+\xi_{43})\xi_{31}]}$$

$$=\frac{1+\xi_{21}+\gamma_4(1+\xi_{43})\xi_{31}}{\lambda_4[(\eta_{12}^2+\xi_{21})\eta_{21}^2+\gamma_4(\eta_{34}^2+\xi_{43})\xi_{31}]}. \tag{21}$$

In terms of variables (20), the averages of the spin variables (14) become

$$\langle\sigma\rangle=\frac{(\eta_{12}^2-\xi_{21}^2)\eta_{24}^2+(\eta_{34}^2-\xi_{43}^2)\xi_{31}^2}{(\eta_{12}^2+\xi_{21}^2)\eta_{24}^2+(\eta_{34}^2+\xi_{43}^2)\xi_{31}^2},$$

$$\langle s\rangle=\frac{(\eta_{12}^2-\xi_{21}^2)\eta_{24}^2-(\eta_{34}^2-\xi_{43}^2)\xi_{31}^2}{(\eta_{12}^2+\xi_{21}^2)\eta_{24}^2+(\eta_{34}^2+\xi_{43}^2)\xi_{31}^2},$$

$$\langle\sigma s\rangle=\frac{(\eta_{12}^2+\xi_{21}^2)\eta_{24}^2-(\eta_{34}^2+\xi_{43}^2)\xi_{31}^2}{(\eta_{12}^2+\xi_{21}^2)\eta_{24}^2+(\eta_{34}^2+\xi_{43}^2)\xi_{31}^2}. \tag{22}$$

It is noteworthy that the symmetry of the system provides the equality $\langle\sigma\rangle=\pm\langle s\rangle$. Without the loss of generality, one can consider that $\langle\sigma\rangle=\langle s\rangle$ hence it appears that at $\langle\sigma\rangle=\langle s\rangle>0$ the right-hand orientation of the averaged vectors $\mathbf{e}_{nm}$ is singled out (see Fig. 1). Then it follows from Eq. (22) that $\eta_{34}=\xi_{43}$. The condition $\langle\sigma\rangle=\langle s\rangle=0$ is met with the

proviso that another equality holds: $\eta_{12}=\xi_{21}$. Since all the fractions in Eqs. (21) should be positive, the equality $\eta_{34}=\xi_{43}$ leads to $\eta_{34}=\xi_{43}=1$, whereas the quantities $\eta_{12}$ and $\xi_{21}$ satisfy the following three-sided inequality: $0<\xi_{21}\leq 1 \leq \eta_{12}$. At $\xi_{21}=\eta_{12}=1$ we have $\langle\sigma\rangle=\langle s\rangle=0$. Thus, the initial system of eight equations (19) in eight unknowns $x_i$, $y_i$ ($i=1, 2, 3, 4$) reduces to the system of four equations, with the unknowns chosen as

$$\rho_1=\xi_{21}, \quad \rho_2=\eta_{12}, \quad \zeta_1=\frac{2a_2}{1+\rho_1}\xi_{31},$$

$$\zeta_2=\frac{a_2}{2}(1+\rho_2)\eta_{24}. \qquad (23)$$

An algebraic transform of Eqs. (21) enables the following representation of the four equations:

$$4\zeta_{1,2}[r+2(\nu_1\nu_2-1)\zeta_{1,2}-\nu_1\nu_2\zeta_{1,2}^2]^2$$
$$-\nu_{2,1}(r-2\zeta_{1,2})(\zeta_{1,2}-2)(r-\nu_{1,2}\zeta_{1,2}^2)^2=0,$$
$$(24)$$

$$\mu_1\equiv\frac{(1+\rho_2)(\rho_1^2-\rho_2)}{(1-\rho_2)(\rho_1^2+\rho_2)}=\frac{\lambda_3\lambda_4}{a_2\lambda_2}\frac{\zeta_2}{\zeta_2-2},$$

$$\mu_2\equiv\frac{(1+\rho_1)(\rho_2^2-\rho_1)}{(1-\rho_1)(\rho_2^2+\rho_1)}=\frac{\lambda_3\lambda_4 a_2}{\lambda_1(r-2\zeta_1)}, \qquad (25)$$

with $2\leq\zeta_{1,2}\leq r/2$ and with the notation

$$r\equiv a_2 b_2\geq 4, \quad \nu_1\equiv\frac{(1+\rho_1)^2(1+\rho_2)}{4(\rho_1^2+\rho_2)},$$

$$\nu_2\equiv\frac{4(\rho_2^2+\rho_1)}{(1+\rho_2)^2(1+\rho_1)}. \qquad (26)$$

First we consider the solutions with $\rho_1=\rho_2=1$ which correspond to the case $\langle\sigma\rangle=\langle s\rangle=0$. For them, the equality $\nu_1=\nu_2=1$ holds and Eqs. (24) are simplified:

$$(r-\zeta_{12}^2)^2(2\zeta_{12}^2-r\zeta_{12}+2r)=0. \qquad (27)$$

At $4\leq r\leq 16$, a single solution is possible:

$$\zeta_1=\zeta_2=r^{1/2}. \qquad (28)$$

By virtue of the equality $\eta_{24}=\xi_{31}$, this solution accounts for the state with $\langle\sigma s\rangle=0$ [see. Eq. (22)]. At $r>16$, another solution with $\zeta_2>\zeta_1$ emerges,

$$\zeta_{2,1}=\frac{1}{4}r^{1/2}[r^{1/2}\pm(r-16)^{1/2}], \qquad (29)$$

which describes the state with $\langle\sigma s\rangle>0$:

$$\langle\sigma s\rangle=\frac{r^{1/2}(r-16)^{1/2}}{r-8}. \qquad (30)$$

The states with $\langle\sigma s\rangle=0$ and $\langle\sigma s\rangle>0$ at $\langle\sigma\rangle=\langle s\rangle=0$ will be referred to as phases I and III (phase II will identify the
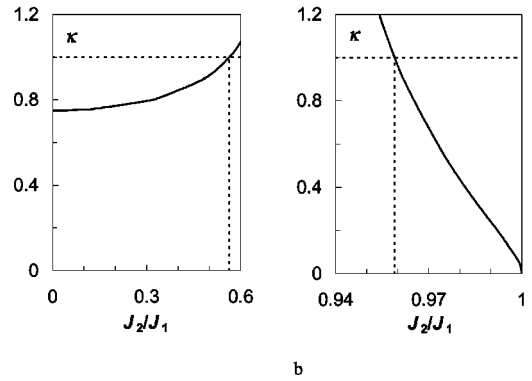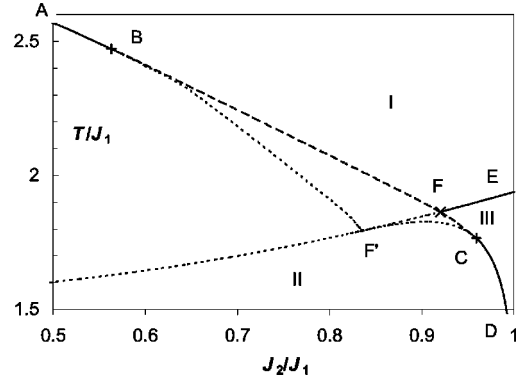


FIG. 3. (a) A section of the phase diagram for two Ising subsystems with fluctuation interactions on the Bethe lattice. Phases I, II, and III respectively imply that $\langle\sigma\rangle=\langle s\rangle=\langle\sigma s\rangle=0$, $\langle\sigma\rangle=\langle s\rangle \neq 0$ at $\langle\sigma s\rangle\neq 0$, and $\langle\sigma s\rangle\neq 0$ at $\langle\sigma\rangle=\langle s\rangle=0$. The phase boundaries I-II, I-III, and II-III are indicated by the lines $ABF$, $FE$, and $FCD$, respectively. The solid lines ($AB$, $FE$, and $CD$) denote second-order transitions, and the dashed line ($BFC$) corresponds to first-order transitions. The lines $ABF'$ and $F'CD$ graphically represent Eq. (40) with regard to Eqs. (37) and (42), the values $\kappa<1$ referring only to the segments $AB$ and $CD$. The line $EFF'$, along with its continuation, is specified by the equation $r=16$. (b) The $J_2/J_1$ dependence of the parameter $\kappa$ calculated by formulas (39) and (43).

state with $\langle\sigma\rangle=\langle s\rangle>0$). The line of the continuous second-order phase transitions I–III defined by the equation $r=16$ is presented in the phase diagram with the axes $T/J_1$ and $J_2/J_1$ [see the line $EFF'$ and its continuation in Fig. 3(a)]. The case $J_2=J_1$ is imaged in this line by the point $E$:

$$\cosh 4K_1=4, \quad T_{\text{I-III}}=\frac{4J_1}{\ln(4+\sqrt{15})}\approx 1.9385 J_1. \qquad (31)$$

In the vicinity of line I-III within phase III, the quantity $\langle\sigma s\rangle$ undergoes a power-law decay with the critical exponent 1/2 [see formula (30)], which agrees with the critical index value for the temperature dependence of the order parameter in the classical "mean-field theory."

We now turn to the analysis of the solutions with $\rho_1<1 <\rho_2$, corresponding to the case $\langle\sigma\rangle=\langle s\rangle>0$ (phase II). Assuming the second-order transitions between phases I and II (at $4\leq r\leq 16$) or III and II (at $r>16$), the variables $\rho_1$ and

$\rho_2$ should continuously approach unity in the vicinity of the lines I-II or III-II within phase II. The limiting behavior of the system of equations (24) and (25) at $\rho_1$, $\rho_2 \to 1$ must therefore be considered in order that the equations of the corresponding lines be found. In so doing, the variables $\rho_1$ and $\rho_2$ are conveniently expressed in terms of $\mu_1$, $\mu_2$ using Eqs. (25):

$$\rho_{1,2} = \frac{2(\mu_{1,2}+1)^2(\mu_{2,1}^2+1)-(\mu_{1,2}-1)^2(\mu_{2,1}+1)^2 \mp \sqrt{D}}{2(\mu_{1,2}+1)^2(\mu_{2,1}^2-1)},$$

$$D = (-1+\mu_1+\mu_2+3\mu_1\mu_2)(1+3\mu_1-\mu_2+\mu_1\mu_2) \quad (32)$$

$$\times (1-\mu_1+3\mu_2+\mu_1\mu_2)(3+\mu_1+\mu_2-\mu_1\mu_2).$$

The limit concerned, $\rho_1$, $\rho_2 \to 1$, corresponds to the region

$$t \equiv 3+\mu_1+\mu_2-\mu_1\mu_2 \geq 0, \quad \mu_1 \geq 1, \quad \mu_2 \geq 1. \quad (33)$$

Indeed, at $t \to 0$ we obtain, accurate to the terms of the order $t$,

$$\rho_1 \approx 1-p\varepsilon+\frac{1}{2}p^2\varepsilon^2, \quad \rho_2 \approx 1+\varepsilon+\frac{1}{2}\varepsilon^2, \quad \varepsilon \ll 1, \quad (34)$$

with the notation

$$\varepsilon \equiv \frac{\sqrt{2t}}{\mu_1+1}, \quad p \equiv \frac{1}{2}(\mu_1-1). \quad (35)$$

Substitution of power series (34) into expressions (26) gives, with the same accuracy,

$$\nu_1 \approx 1-\frac{1}{4}p(p+2)\varepsilon^2, \quad \nu_2 \approx 1+\frac{1}{4}(1+2p)\varepsilon^2. \quad (36)$$

Now it is possible to approximately solve the system of equations (24) with respect to the variables $\zeta_1$ and $\zeta_2$, and to insert the expressions derived into Eqs. (25) so as to find the variables $\mu_1$ and $\mu_2$. The latter afford, with definitions (33) and (35), a closed equation in the small parameter $\varepsilon$. Since the system of equations (24) has, in a zero-order approximation in $\varepsilon$, two solutions [Eqs. (28) and (29)], depending on the parameter $r$, we separately discuss the cases $4 \leq r \leq 16$ and $r > 16$. The two intervals of the values $r$ respectively refer to phase transitions I-II and III-II.

At $4 \leq r \leq 16$ we deduce

$$\zeta_{1,2} \approx r^{1/2}-\frac{1}{2}\frac{r^{1/2}-2}{4-r^{1/2}}[2\nu_{2,1}'-(r^{1/2}-2)\nu_{1,2}']\varepsilon^2,$$

$$\mu_{1,2} \approx f_{1,2}\left[1\pm\frac{2(\nu_1'+\nu_2')-r^{1/2}\nu_{2,1}'}{r^{1/2}(4-r^{1/2})}\varepsilon^2\right]$$

$$f_1 \equiv \frac{r^{1/2}(r^{1/2}+2)}{a_2\lambda_2}, \quad f_2 \equiv \frac{a_2(r^{1/2}+2)}{r^{1/2}\lambda_1}, \quad \nu_{1,2}' \equiv \left(\frac{\partial \nu_{1,2}}{\partial \varepsilon^2}\right)_{\varepsilon=0}. \quad (37)$$

The solution of the equation in $\varepsilon$ can be written as

$$\varepsilon^2 = \frac{2}{(f_1+1)^2(1-\kappa)}t, \quad (38)$$

$$\kappa = \frac{2(1-p^2)(f_1-f_2)+r^{1/2}[3(1+4p+p^2)+p(p+2)f_1+(1+2p)f_2]}{2r^{1/2}(4-r^{1/2})(f_1+1)^2}. \quad (39)$$

The quantities $t$ and $p$ are determined by relations (33) and (35), with the values $f_1$ and $f_2$ from Eq. (37) substituted for $\mu_1$ and $\mu_2$. According to solution (38), the second-order transition I-II occurs if

$$t = 3+f_1+f_2-f_1f_2 = 0 \quad (40)$$

provided that the coefficient $\kappa$ falls within the range from 0 to 1. The lines defined by Eqs. (40) and $r=16$ [see the lines $ABF'$ and $EFF'$ in Fig. 3(a)] intersect at the point $F'$ ($J_2/J_1=0.8353$, $T/J_1=1.7938$). At the left, Fig. 3(b) shows the $J_2/J_1$-dependence of the coefficient $\kappa$ along the line $ABF'$ given by Eq. (40). The value $\kappa=1$ is found at point $B$ ($J_2/J_1=0.5633$, $T/J_1=2.4725$). As a result, the second-order transition I-II can be realized on the interval $0 \leq J_2/J_1 \leq 0.5633$ [line $AB$ in Fig. 3(a)]. On substituting $\rho_1$, $\rho_2$ and $\zeta_1$, $\zeta_2$ as power series in $\varepsilon$ [see Eqs. (34) and (37)] into relations (22), we obtain, with designations introduced in Eq. (23):

$$\langle\sigma\rangle = \frac{1}{2}(1+p)\varepsilon, \quad \langle\sigma s\rangle = \frac{1+4p+p^2}{4(4-r^{1/2})}\varepsilon^2,$$

$$\langle\sigma s\rangle - \langle\sigma\rangle^2 \geq 0. \quad (41)$$

From relations (33), (38), and (40) it follows that the parameter $t$ is proportional to the temperature difference $T_c-T$ [$T$ is the temperature within phase II; $T_c$ is the temperature of the phase transition I-II which obeys Eq. (40)] and the parameter $\varepsilon$ is proportional to $t^{1/2}$. To put it another way, the quantity $\langle\sigma\rangle$ in phase II in the vicinity of the I-II phase boundary tends to zero with the critical exponent 1/2, which is in agreement with the temperature dependence of the order parameter in the mean-field approximation. For the quantity $\langle\sigma s\rangle$, the corresponding critical exponent is equal to 1. In the limit $t \to 0$ with $J_2=0$, we arrive at: $p=1, r^{1/2}=5/2$ and $\langle\sigma s\rangle = \langle\sigma\rangle^2 = \varepsilon^2 = t/2$, where $t = 16(1-2z)$, $z \equiv \exp(-2K_1)$. This is consistent with the results of the Ising model on the Bethe lattice[10] which implies the following tempera-

ture dependence for the averages of the statistically independent spins $\sigma$ and $s$ in the ordered phase: $\langle\sigma\rangle=(1-4z^2)^{1/2}/2(1-2z^2)$.

Figure 4(a) demonstrates the order parameters $\langle\sigma\rangle$ and $\langle\sigma s\rangle$, the quantity $\langle\sigma s\rangle-\langle\sigma\rangle^2$, and the specific heat $C$ against temperature. The value of the parameter $J_2/J_1$ is put equal to 1/3 as is the case in realistic dipole-dipole interactions. To evaluate the temperature dependences of the order parameters (22), the system of equations (21) was solved numerically, and the specific heat was found by numerical differentiation of expression (13). Note that the quantity $\langle\sigma s\rangle-\langle\sigma\rangle^2$ behaves nonmotonically and the specific heat undergoes a jump at the transition point (at $T/J_1=2.751$), which is typical of the mean-field approximation.

Passing on to the analysis of the second-order transitions II-III occurring at $r>16$, we rewrite relations (37):

$$\zeta_{1,2}\approx\zeta_{1,2}^{(\mathrm{III})}\left[1+4\frac{r\nu'_{2,1}-8(\nu'_1+\nu'_2)}{r(16-r)}\varepsilon^2\right],$$

$$\mu_{1,2}\approx f_{1,2}\left[1+2(\zeta_1^{(\mathrm{III})}-2)\frac{r\nu'_{1,2}-8(\nu'_1+\nu'_2)}{r(16-r)}\varepsilon^2\right],$$

$$f_1\equiv\frac{(r-4)\zeta_1^{(\mathrm{III})}}{2a_2\lambda_2},\quad f_2\equiv\frac{a_2(r-4)}{2\lambda_1\zeta_2^{(\mathrm{III})}},\quad \nu'_{1,2}\equiv\left(\frac{\partial\nu_{1,2}}{\partial\varepsilon^2}\right)_{\varepsilon=0},\tag{42}$$

where $\zeta_{2,1}^{(\mathrm{III})}$ refer to values (29) for phase III. Equation (38) holds the same form, with the value $f_1$ specified by Eq. (42) and with the parameter $\kappa$ expressed differently:

$$\kappa=\frac{\zeta_1^{(\mathrm{III})}-2}{r(f_1+1)^2}\left\{\frac{[(1+2p)f_1-p(p+2)f_2]r+8(p^2-1)(f_1+f_2)}{r-16}-3(p^2-1)\right\}.\tag{43}$$

The second-order transition III-II is realized subject to the same condition (40), provided that the coefficient $\kappa$ falls within the range from 0 to 1 [see the line $F'CD$ in Fig. 3(a) and the right-hand part in Fig. 3(b)] but the value $\kappa=1$ is now realized at the point C ($J_2/J_1=0.9590$, $T/J_1=1.7663$). Hence it is obvious that the second-order transition III-II can take place on the interval $0.9590\leqslant J_2/J_1\leqslant1$ [see the line $CD$ in Fig. 3(a)]. The following relation should be substituted for Eq. (41):

$$\langle\sigma\rangle=\frac{1+p}{1+(\zeta_1^{(\mathrm{III})}/\zeta_2^{(\mathrm{III})})^2}\varepsilon,$$

$$\langle\sigma s\rangle-\langle\sigma s\rangle_{\mathrm{III}}=\frac{8(1+4p+p^2)}{(r-8)(r-16)}\varepsilon^2,\tag{44}$$

[here $\langle\sigma s\rangle_{\mathrm{III}}$ is determined by expression (30) for phase III]. The critical exponents for these order parameters are the same as in phase II at $4\leqslant r\leqslant16$. To illustrate the temperature dependences of thermodynamic values on the interval concerned, we have chosen the value $J_2/J_1=0.97$ [see Fig. 4(c)]. Two second-order phase transitions proceed at the temperatures $T_{\mathrm{II-III}}/J_1=1.73$ and $T_{\mathrm{III-I}}/J_1=1.92$, either being accompanied by a jump of specific heat.

As the parameter $J_2/J_1$ approaches unity, the phase transition temperature goes to zero. At $J_2/J_1\rightarrow1$, Eq. (40) becomes simpler:

$$T_{\mathrm{II-III}}\approx\frac{8J_1}{\ln[\gamma T_{\mathrm{II-III}}/(J_1-J_2)]},\quad\gamma=\frac{3}{4},\quad J_2\rightarrow J_1.\tag{45}$$

Equation (45) is identical in form to the Ising-model asymptotic equation in transition temperature for a square lattice, with interactions along either horizontal or vertical

bonds tending to zero; such vanishing interaction is modeled by the difference $J_1-J_2$ entering into the above equation. The only distinction is in the coefficient values, and it arises, first, from the specificity of the model in question which involves two spin sublattices and, second, from the fact that the fluctuation interaction is intrinsically given less weight for the Bethe lattice than for a square lattice. If $J_2/J_1=1$, the ground state with the structure of phase II exists only at zero temperature. An infinitesimal increase in temperature immediately brings the system into phase III which persists up to the temperature $T_{\mathrm{I-III}}$ found from Eq. (31). In the next section, we consider this special case when the spin interaction constant within one subsystem is the same as between two subsystems and demonstrate that this peculiarity enables exact calculation of the partition function not only for the Bethe lattice but for a square lattice as well.

In the previously published communication,[17] a simplified analysis of the system of equations (21) was performed which enabled Eq. (40) to be derived and interpreted as an equation accounting for second-order transitions to phase II without any limitations. It followed from the paper that phase II was separated from phases I and III by the lines $ABF'$ and $F'CD$, respectively [see Fig. 3(a)]. In fact, the line of second-order transitions to phase II has its extremities at the points B and C. On the other hand, the numerical analysis of the system of equations (21) [or (24) and (25)] suggests that only first-order transitions to phase II can happen between the points B and C (i.e., on the interval $0.5633\leqslant J_2/J_1\leqslant0.9590$)—see the dashed line in Fig. 3(a). This line has common tangents with the lines $AB$ and $CD$ at points $B$ and $C$, respectively, in accord with the properties of critical points between the lines of first-order and second-order phase transitions in terms of the Landau theory.[18] Now phase II has a boundary with phase I along the line $ABF$ and
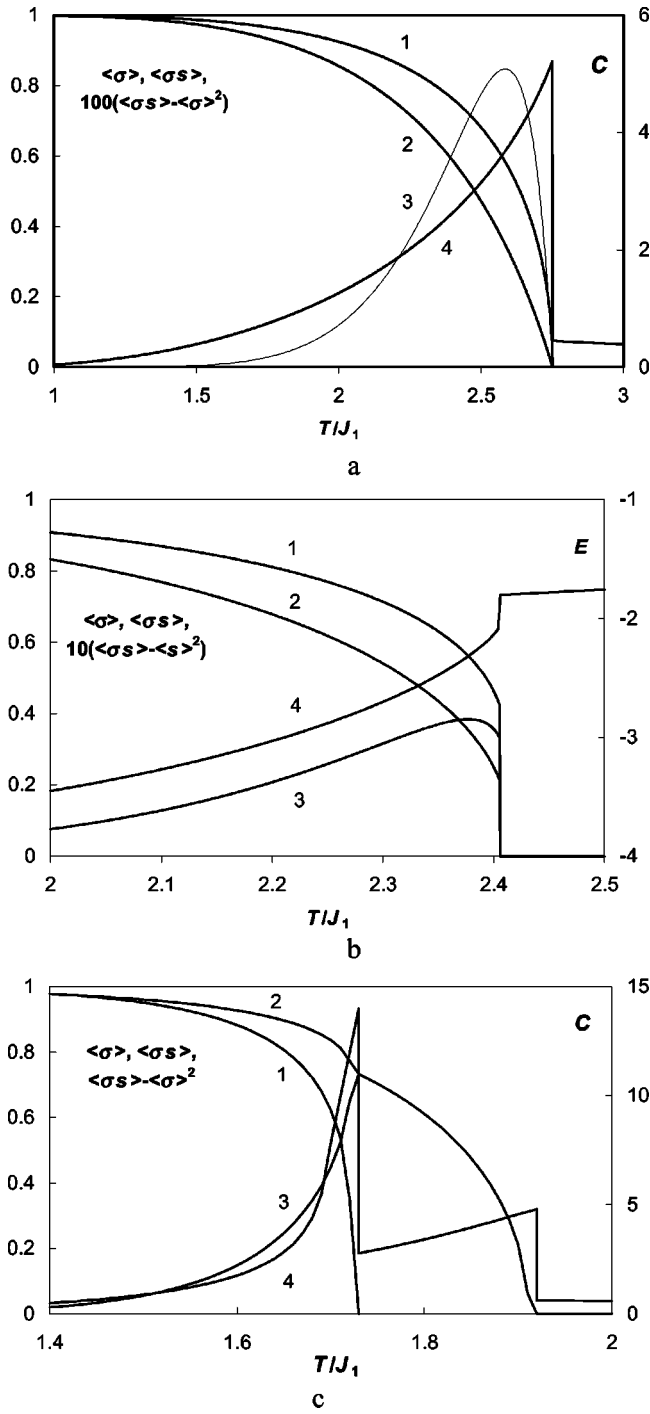
FIG. 4. Temperature dependences of the thermodynamic characteristics for the system under study on the Bethe lattice at $J_2/J_1 = 1/3$ (a), 0.6 (b), and 0.97 (c). The lines 1, 2, and 3 (see the left-hand axis of ordinates) correspond to the values $\langle \sigma \rangle = \langle s \rangle$, $\langle \sigma s \rangle$, $\langle \sigma s \rangle - \langle \sigma \rangle^2$; the line 4 (see the right-hand axis of ordinates) represents specific heat $C$ [(a), (c)] or energy $E$ (b).
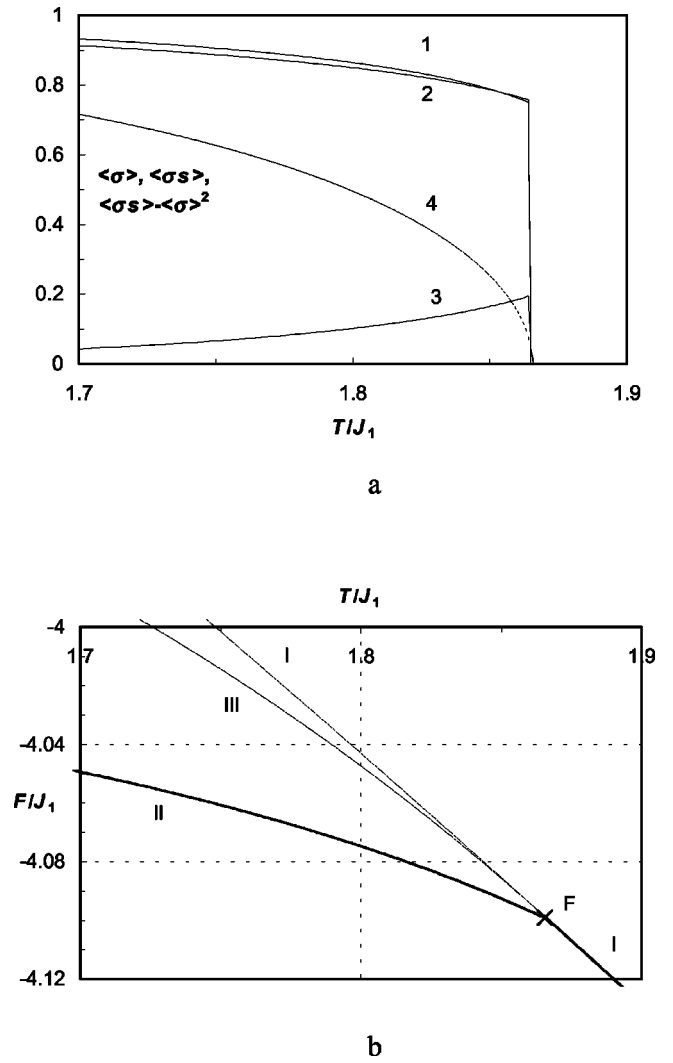


FIG. 5. Temperature dependences of the thermodynamic characteristics in the cross-section of the phase diagram by the line $J_2/J_1 = 0.92$ which includes the triple point. (a) The lines 1, 2, and 3 indicate the respective order parameters $\langle \sigma \rangle = \langle s \rangle$, $\langle \sigma s \rangle$, and $\langle \sigma s \rangle - \langle \sigma \rangle^2$ in phase II, and the line 4 represents $\langle \sigma s \rangle$ in phase III. (b) Free energies of phases I, II, and III.

with phase III along the line $FCD$. The point $F$ at which the three phases coexist is defined by the coordinates $J_2/J_1 \approx 0.92$ and $T/J_1 \approx 1.87$. The temperature dependences of the order parameters and free energies for these phases are presented in Fig. 5 at the fixed value $J_2/J_1$ corresponding to point $F$. Lines III and I have a common tangent at this point,

while the lines II and I join with a dog leg. Accordingly, transition III-I is characterized by a jump solely in specific heat, and the transition II-I implies an energy jump [see, for instance, line 4 in Fig. 4(b)]. The only (first-order) transition occurs in the range $0.5633 < J_2/J_1 < 0.92$ [as in Fig. 4(b)], and two (first-order and second-order) transitions fall within the range $0.92 < J_2/J_1 < 0.9590$.

## IV. PHASE TRANSITIONS ON A SQUARE LATTICE

The results obtained in the previous section for the Bethe lattice with the coordination number 4 can be regarded as a cluster approximation of the model on a square lattice described by Hamiltonian (3). Distinctions between the two approaches are due to the fact that the cluster approximation neglects the interactions of order-parameter fluctuations at a distance longer than the cluster size. In the trivial special
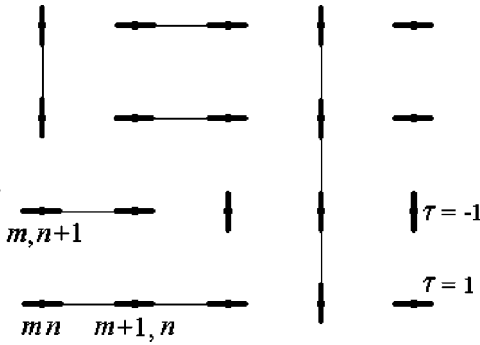
FIG. 6. A sample distribution of spin variables over the sites of a square lattice. For the case $J_1 = J_2$, the solid lines connect the coupled $\sigma$ spins which provide the energy contribution of $\pm 4J_1$ (the sign is governed by the values of $\sigma$ variables). Upon the summation over the states of $\sigma$ spins, the energy of effective interactions in the pairs of neighboring $\tau_1$ and $\tau_2$ spins appears as $-\tilde{J}\tau_1\tau_2$, where $\tilde{J} = (T/4)\ln(\cosh 4J_1/T)$ (see the explanation in the text).

case free of fluctuation interactions ($J_2 = 0$), it is possible to compare the results gained by the cluster approximation and the 2D Ising model for either of spin subsystems. For example, the phase transition temperature is equal to $2.8854J_1$ for the Bethe lattice and to $2.2692J_1$ for a square lattice. It turns out that the case $J_1 = J_2$ also admits of an exact solution on a square lattice. To find this solution, introduce the new spin variables $\tau_{mn} = \sigma_{mn} s_{mn}$ and rewrite Hamiltonian (3) as

$$H = -\sum_{mn} \{[(1 + \tau_{mn}\tau_{m+1,n})J_1$$

$$+ (\tau_{mn} + \tau_{m+1,n})J_2]\sigma_{mn}\sigma_{m+1,n} + [(1 + \tau_{mn}\tau_{m,n+1})J_1$$

$$- (\tau_{mn} + \tau_{m,n+1})J_2]\sigma_{mn}\sigma_{m,n+1}\}. \quad (46)$$

At $J_1 = J_2$ the bracketed expressions can assume only two values, $4J_1$ and 0. The former corresponds to the horizontal bond with $\tau_{mn} = \tau_{m+1,n} = 1$ or the vertical bond with $\tau_{mn} = \tau_{m,n+1} = -1$. The zero value results in all other cases. As a consequence, the diagram expansion of the partition function over the $\sigma$ spins[18] [which involves the identity $\exp(a\sigma) = \cosh a + \sigma \sinh a$, $\sigma = \pm 1$] will include only horizontal and vertical chains having no common sites (see Fig. 6). The subsystem of $\sigma$ spins thus becomes quasi-one-dimensional, the long-range order vanishing ($\langle\sigma\rangle = 0$). Hence, the summation over $2^N$ states of $\sigma$ spins will nullify all the summands containing at least one hyperbolic sine among cofactors and we arrive at the following partition function:

$$Z = \sum_{\{\tau\},\{\sigma\}} \exp(-H/T)$$

$$= 2^N \sum_{\{\tau\}} \prod_{mn} \{[\cosh(1 + \tau_{mn})(1 + \tau_{m+1,n})K_1]$$

$$\times [\cosh(1 - \tau_{mn})(1 - \tau_{m,n+1})K_1]\} \quad (47)$$

($K_j = J_j/T, j = 1,2$). Since the hyperbolic cosine arguments take on only two values, $4K_1$ and 0, we involve the identity

$$\cosh(1 \pm \tau_1)(1 \pm \tau_2)K_1 = \exp[(1 \pm \tau_1)(1 \pm \tau_2)\tilde{K}],$$

$$\tilde{K} = \frac{1}{4}\ln(\cosh 4K_1) \quad (48)$$

to reduce the partition function to the form

$$Z = 2^N(\cosh 4K_1)^{N/2} Z_{\text{Ising}}(\tilde{K}). \quad (49)$$

Here $Z_{\text{Ising}}(\tilde{K})$ designates the partition function of the 2D Ising model with the effective Hamiltonian

$$H_{\text{eff}} = -\tilde{J}\sum_{mn} [\tau_{mn}\tau_{m+1,n} + \tau_{mn}\tau_{m,n+1}], \quad \tilde{J} = T\tilde{K}, \quad (50)$$

in which the temperature-dependent interaction constant $\tilde{J}$ accounts for the thermodynamically averaged coupling of two $\sigma$-neighboring spins. The temperature of the phase transition from the disordered ($\langle\tau\rangle = 0$) to the ordered ($\langle\tau\rangle \neq 0$) state corresponding to the appearance of the nonequivalent $x$ and $y$ directions is derived from the equation $\sinh 2\tilde{K}_c = 1$ for the critical temperature of the 2D Ising model:

$$\cosh 4K_1 = 3 + 2\sqrt{2}, \quad T_{\text{I-III}} = 1.6337J_1. \quad (51)$$

A comparison of relations (51) and (31) shows that the value $T_{\text{I-III}}$ for a square lattice is smaller than that for the Bethe lattice in accordance with the tendency for the cluster approximation (resulting from the Bethe-lattice treatment) to overestimate the transition temperature.

Turning to the analysis of the phase diagram in the region where the fluctuation interaction constant has intermediate values ($0 \leqslant J_2 \leqslant J_1$), it should be noted first of all that the chains of $\sigma$ spins (see Fig. 6) become coupled at $J_2 \rightarrow J_1$, since one of the bracketed expressions in Eq. (46) assumes a nonzero value, $2(J_1 - J_2)$, and a spontaneous polarization thus arises in the system. The temperature $T_{\text{II-III}}$ of the phase transition into the state with $\langle\sigma\rangle \neq 0$ is given by Eq. (45) with the numerical coefficient $\gamma$ of the order of unity. On the other hand, the value $T_{\text{I-III}}$ specified by formula (51) remains practically unchanged in the vicinity of the point $J_2/J_1 = 1$. As a consequence, phase III with $\langle\tau\rangle \neq 0$ is now intermediate in temperature between phases I and II. It is also evident that with the decreasing parameter $J_2$, the lines of phase transitions I-III and III-II will intersect at a triple point where $T_{\text{I-III}} = T_{\text{II-III}}$. These qualitative speculations are corroborated by the analytical solutions of the same problem for the corresponding Bethe lattice (see Sec. III).

Using a Monte Carlo simulation, it becomes possible to include the region of intermediate values of the fluctuation interaction constant ($0 \leqslant J_2 \leqslant J_1$) into the phase diagram. To this end, the Metropolis algorithm[19] at decreasing temperature was employed. The system under study was represented by a square cluster with the linear dimension $La$ ($a$ is the lattice constant) and the periodic boundary conditions. To reach the thermodynamic equilibrium and to average the quantities of interest, we used the Markov chains with the length of the order $10^5$ and $10^6 - 10^7$ steps per lattice site, respectively. A plausible statistic for the Hamiltonian con-
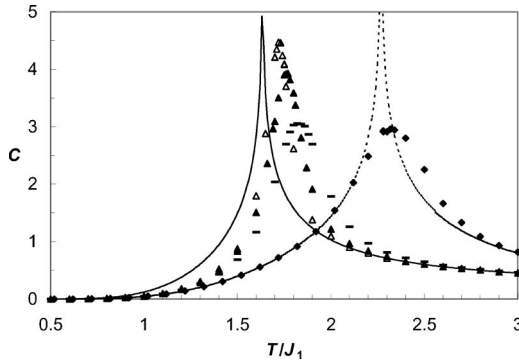
FIG. 7. Temperature dependences of specific heat calculated from the exact expressions for the free energy (lines) and from the Monte Carlo computational data [$L=14$ (filled triangles and diamonds), $L=10$ (dashes), and $L=18$ (empty triangles)] for the cases $J_2/J_1=0$ (the dashed line and diamonds) and $J_2/J_1=1$ (the solid line as well as triangles and dashes).

cerned in the critical region was gained with the number of steps two orders of magnitude larger than in the absence of fluctuation interactions (see, e.g., Ref. 20). The phase transition temperatures were determined from the peaks of specific heat and also from the inflection points of the temperature dependences of $\langle \sigma \rangle$ and $\langle \sigma s \rangle$, both approaches being in nice accordance. The $L$-dependence of the thus found transition temperatures was studied for the cases $J_2=0$ and $J_2=J_1$ admitting of the exact solutions. For $L=14$, the phase transition temperatures proved to be about $0.1\,J_1$ above the exact values for the corresponding infinite system. Figure 7 demonstrates the agreement between the temperature dependence of specific heat found from the exact expression for the free energy and that provided by the Monte Carlo simulation.

To construct a phase diagram in a wide range of the values $0 \leq J_2 \leq J_1$, we involved a cluster with $L=14$, which enabled a compromise between the computer time and the calculation accuracy. The simulation results presented in Fig. 8 support the occurrence of the triple point and the appearance of a new phase III, and also furnish a good approximation of the I-II and I-III phase transition temperatures. The computational difficulties, however, emerged in modelling the III-II transition at the values $J_2$ close to $J_1$, since the system "froze" in phase II. This may be attributable to an underestimated probability of the III-II transition in a cluster of the given size which causes a distortion of the distribution function. The same effect is also likely to account for the systematically underestimated values of specific heat in phase III at $J_2=J_1$, in contrast to the case $J_2=0$ when the low-temperature shoulder of the specific heat was reproduced practically exactly (see Fig. 7). This impediment can be surmounted using cluster algorithms (like that developed in Ref. 21 for the Potts model).

Figure 8 also includes the line of phase transition I-II which is specified by the equation $\sinh^4 2K_1 - \sinh^4 2K_2 = 1$ [resulting from the duality transformation—see Eq. (21) at $K_3=0$ in Ref. 13] and agrees well with the corresponding Monte Carlo computational data within the accuracy of the method. Clearly, this line cannot describe the phase boundary
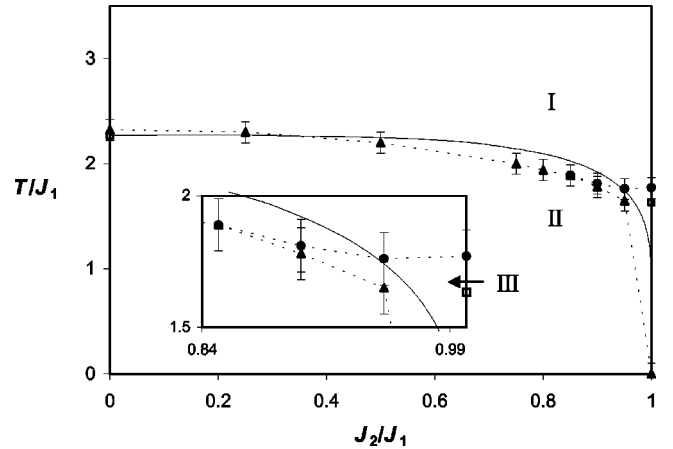


FIG. 8. The phase diagram of the two Ising subsystems with fluctuation interactions on a square lattice. Phases I, II, and III are the same as in Fig. 3(a). The vicinity of the point at which the three phases coexist is shown on an enlarged scale in the box. Triangles and circles with error bars connected with dotted lines indicate the transitions to phase II and between phases I and III (the result of Monte Carlo simulation for $L=14$). Empty squares at $J_2/J_1=0$ and 1 correspond to the exact calculation of the partition function. The solid line corresponds to the duality transformation (as presented in Ref. 13), $\sinh^4 2K_1 - \sinh^4 2K_2 = 1$, for the phase transitions I-II.

II-III, just as the duality transformation within the Ashkin-Teller model fails to reveal the phase with $\langle \sigma s \rangle \neq 0$, $\langle \sigma \rangle = \langle s \rangle = 0$.

## V. DISCUSSION

Phase diagrams constructed on a square lattice and on the Bethe lattice with the coordination number 4 strongly evidence for the occurrence of phase III at the values $J_2$ close to $J_1$. Phase III corresponds to the average values $\langle \sigma s \rangle \neq 0$, $\langle \sigma \rangle = \langle s \rangle = 0$ and resembles, in this sense, one of the phases involved in the Ashkin-Teller model.[9,10] For the quasidipole systems considered here this phase represents a new type of orientational ordering. Using the relationship between the unit vectors $\mathbf{e}_{mn}$ and spin variables [see Eq. (2)], it is readily shown that phase III with $\langle \sigma s \rangle \neq 0$ implies the nonequivalent mean-square projections $\langle (e_{mn}^x)^2 \rangle = (1+\langle \sigma s \rangle)/2$ and $\langle (e_{mn}^y)^2 \rangle = (1-\langle \sigma s \rangle)/2$ in the absence of spontaneous polarization ($\langle e_{mn} \rangle = 0$). Thus, the $x$ and $y$ axes become inequivalent in the system.

An exact solution as such is of value in the theory of critical phenomena (where only a few exact results are available) and generally provides a new insight into the physics of the system under study. So does the exact solution considered in Sec. IV: it gives the clue to the mechanism by which phase III arises.

Indeed, with the condition $J_2/J_1=1$, one of the spin subsystems (the subsystem $\sigma$, specifying the left-right or up-down direction of the unit vector $e_{mn}$) becomes quasi-one-dimensional; as a consequence, the other one (the subsystem $\tau = \sigma s$, specifying the horizontal or vertical alignment of the unit vector $\mathbf{e}_{mn}$) is describable by the effective Hamiltonian

of the 2D Ising model, but with a peculiar (temperature-dependent) interaction constant averaged over the spins of the first subsystem (see Fig. 6). At $J_2/J_1 \to 1$, the quasi-one-dimensionality of the first subsystem vanishes and the system is characterized by two phase transitions at non-zero temperatures $T_{\text{I-III}}$ and $T_{\text{II-III}}$ [see Eqs. (51) and (45) with the numerical coefficient $\gamma$ of the order of unity]. Thus, phase III results from the quasi-one-dimensionality of one of the spin subsystems. At the values $J_2/J_1$ strongly deviating from unity, the prerequisites for the phase III occurrence disappear.

We now turn to the possibility for phase III to be detected experimentally. For systems with real dipole-dipole interactions, the ratio $J_2/J_1 = 1/3$ is strictly specified and phase III cannot be realized. Consider a system of nonpolar molecules with quasinormal orientations relative to the lattice of adsorption centers. It was shown previously[13] that in this case the angular dependences of quadrupole-quadrupole, dispersion, and repulsive interactions are described well by the Hamiltonian of dipole-dipole interactions, with the renormalized constants $D_1$ and $D_2$ [see Eq. (1)]. Below are the explicit dependences of the parameters $J_1$ and $J_2$ as well as the parameter $J_4$ of the Ashkin-Teller model [see Eq. (4)] on the constants of quadrupole-quadrupole and dispersion interactions (repulsive interactions are not treated here, since they are negligible for the real adsorption systems in which intermolecular separations are governed by the lattice of adsorption centers and far exceed the equilibrium values in the gas-phase dimers).

$$J_1 = \left(\frac{15}{4}U - \frac{3}{2}W\right)\cos^2\theta\sin^2\theta,$$

$$J_2 = \left(\frac{9}{4}U - \frac{1}{2}W\right)\cos^2\theta\sin^2\theta,$$

$$J_4 = -\left(\frac{57}{16}U - \frac{5}{2}W\right)\sin^4\theta, \quad U = \frac{Q^2}{a^5}, \tag{52}$$

$$W = \frac{\hbar}{2\pi a^6}\int_0^\infty [\chi_\parallel(i\omega) - \chi_\perp(\omega)]^2 d\omega.$$

Here $Q$ is the molecular quadrupole moment, $a$ is the intermolecular distance (the lattice constant), $\chi_\parallel(\omega)$ and $\chi_\perp(\omega)$ designate polarizability components longitudinal and transverse with respect to the long molecular axis. For quasinormal orientations, the value $J_4$ is small by virtue of the small angle $\theta$ at which the molecules are inclined to the surface-normal direction. As an example, the energy of quadrupole-quadrupole interaction in the system CO/NaCl(100), $U \approx 1.63$ meV, is more than three times as large as the energy of anisotropic component of dispersion interaction, $W \approx 0.5$ meV, and exceeds by more than ten times the energy of dipole-dipole interactions (due to the smallness of the dipole moment of the molecule CO). Even a relatively large value of the angle $\theta$ (about 25°) for this system[16] affords a sufficient smallness of the value $J_4$ ($J_4/J_1 \approx -0.2$). The ratio $J_2/J_1$ does not depend on $\theta$ and approximately equals

0.64 (only for quadrupole-quadrupole interactions, $J_2/J_1 = 0.6$). Phase III therefore cannot result for the system CO/NaCl(100) and the orientational transition observed at the temperature $T_c = 17.5 \div 21.5$ K (Ref. 22) occurs in this system between phases I and II. The Monte Carlo simulation performed by us provides the phase transition temperature $T_\sigma$, which falls within the same temperature range.

The values of numerical coefficients for the parameters $J_1$ and $J_2$ in Eqs. (52) merit notice. The equality $J_1 = J_2 > 0$ holds at $W = (3/2)U$. As a consequence, there are no fundamental obstacles to the realization and experimental observation of phase III: it can be detected provided dispersion interactions are strong in comparison with quadrupole-quadrupole interactions. This becomes quite plausible, e.g., for the molecules with high polarizabilities and small quadrupole moments or with relatively small molecular separations.

In summary, systems with fluctuation interactions represent a discrete counterpart of a more populated class of systems with the continuously degenerate ground state. At the same time, Hamiltonian (3) is remarkable not only for its specific applications in the description of the orientational states for adsorbates, but because it underlies a fruitful model in phase transition theory. It is not so sophisticated in structure as the spin representation of the eight-vertex model,[10] implies three phases, and enables (at a certain parameter ratio) an exact calculation of the partition function. We have constructed the full phase diagram by Monte Carlo modeling and also using the equivalent Bethe lattice (as shown in Ref. 23, calculations on a Bethe lattice are more reliable than conventional mean-field calculations, the latter being quite inapplicable to the model concerned here). These findings clearly demonstrate the occurrence of an intermediate phase state and thus represent a great stride toward understanding the nature of the systems with continuously degenerate ground states. Such systems might be expected to have a state similar to phase III and an effect of "ordering due to disorder" with more fascinating features than commonly supposed. This conjecture is supported by the appearance (in a very narrow parameter range) of the short-range-ordered phase without polarization in the context of the strict dipole model ($J_2/J_1 = 1/3$).[15] Thus it is tempting to extend the analysis to the continuously quasidipole case with $J_2/J_1 \to 1$, as it may reveal a more clearcut analog of phase III. It is also promising to study the Ashkin-Teller model with allowance made for the newly introduced fluctuation interactions, i.e., to superpose Hamiltonians (3) and (4). Such a combined treatment should furnish an even more intriguing phase diagram than either of the two individual models and will be particularly helpful in the analysis of orientational states of adsorbates.

## APPENDIX. GENERAL FORM OF THE FREE ENERGY FOR AN ARBITRARY-SPIN ANISOTROPIC MODEL ON THE BETHE LATTICE

The Bethe lattice is regarded as a convenient tool in studies on ''spinlike'' systems since it enables recurrent relations for the equations of states for such systems to be introduced and also provides qualitatively correct results.[23] The Bethe lattice is the infinite ''interior'' of the infinite Cayley tree which is characterized by the large contribution from the boundary ''surface'' nodes. Thus, the latter cause a great effect on the thermodynamic properties[24,25] and make them behave differently than in the ''interior'' which is just the focus of our attention. Intensive quantities are rather easy to derive from the stable point of the recurrent equations of state, whereas the calculation of extensive quantities encounters certain difficulties associated with eliminating the outer part of the Cayley tree and also with choosing the correct ratio ($q/2$) of the number of bonds to the number of sites for the Bethe lattice with the coordination number $q$. To surmount these difficulties, one has to invoke some auxiliary techniques, for instance, to integrate the equations of states over the external field so as to obtain the free energy of the system.[10] A straightforward geometrical method for calculating the free energy of the Bethe lattice was proposed previously.[23] A similar result can also be obtained by a ''more transparent'' algebraic approach.[26,27] Though intuition suggests that these results should be independent of whether spin coupling constants are isotropic or anisotropic along different bonds on the Bethe lattice, it is nevertheless expedient to derive the relations concerned for the anisotropic model. Moreover, the derivation proposed here is concise and free of any additional assumptions (used, e.g., in Ref. 27), and it yields a remarkably brief and easy-to-apply form of the final expression for the free energy and the corresponding equation of state. This general result for an arbitrary-spin anisotropic model is exemplified by a compact derivation of the free energy in the anisotropic Ising model on the Bethe lattice. We use the same general relations also in Sec. III to analyze the states of the system with fluctuation interactions.

Consider a Cayley tree (see Fig. 9) with the nodes each containing the spin $\sigma$ which takes on $2s+1$ values ($\sigma = -s, -s+1, ..., s-1, s$). We begin the analysis at the so-called central node surrounded by $N$ shells which is bound to $q$ branches labeled in the same way as the corresponding bonds, *viz.* by the index $j=1, 2, ..., q$, where $q$ is the coordination number of the tree. (For the anisotropic model involved here, the interaction constants for different bonds are assumed different.) With the spin at the central node denoted by $\sigma_0$, the partition function of the spin system on a given Cayley tree can be written as follows:

$$Z_N = \sum_{\sigma_0} W(\sigma_0) \prod_{j=1}^{q} g_N^{(j)}(\sigma_0). \tag{A1}$$

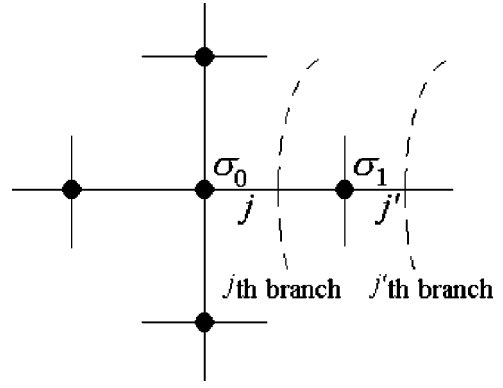

FIG. 9. The central part of the Cayley tree with the coordination number $q=4$. The central node at which the spin $\sigma_0$ resides is bound to four branches labeled by the index $j=1, 2, 3, 4$. The spin $\sigma_1$ is positioned at the node incident to the bond $j$ and three bonds $j'$.

Here $W(\sigma_0)$ designates the Boltzmann weight for the interaction between $\sigma_0$ and external fields, and $g_N^{(j)}(\sigma_0)$ is the restricted partition function obtained by summing over all spins belonging to the $j$th branch of the Cayley tree in each of $N$ shells (see Fig. 9). The recurrence equation relates the quantity for the $j$th branch in the innermost shell, $g_N^{(j)}(\sigma_0)$, to that for the $j'$th branch in the next shell, $g_{N-1}^{(j')}(\sigma_1)$ (the spin $\sigma_1$ is positioned at the node incident to the $j$th bond and $q-1$ $j'$th bonds):

$$g_N^{(j)}(\sigma_0) = \sum_{\sigma_1} W_j(\sigma_0, \sigma_1) \prod_{j'(\neq j)} g_{N-1}^{(j')}(\sigma_1). \tag{A2}$$

$W_j(\sigma_0, \sigma_1)$ denotes the Boltzmann weight for the $j$th bond which is contributed by the coupling between the spins $\sigma_0$ and $\sigma_1$ as well as by the interaction between $\sigma_1$ and external fields.

At $N \gg 1$, the extensive quantities $g_N^{(j)}(\sigma_0)$ can be represented as the products of the extensive quantity $\zeta_N^{(j)}$ (depending on $N$ but not on $\sigma_0$) and the intensive quantity $z^{(j)}(\sigma_0)$ (independent of $N$):

$$g_N^{(j)}(\sigma_0) = \zeta_N^{(j)} z^{(j)}(\sigma_0). \tag{A3}$$

[The treatment of the isotropic system[27] involved, instead of $\zeta_N^{(j)}$, the analogous quantities irrespective of $j$ which were put equal to $g_N(s)$.] Then the quantities $z^{(j)}(\sigma_0)$ are defined by the system of equations

$$z^{(j)}(\sigma_0) = [\Psi_{N-1}^{(j)}]^{-1} \sum_{\sigma_1} W_j(\sigma_0, \sigma_1) \prod_{j'(\neq j)} z^{(j)}(\sigma_1), \tag{A4}$$

in which $\Psi_{N-1}^{(j)}$ can be regarded as the coefficients of the recurrent relationships for $\zeta_N^{(j)}$:

$$\zeta_N^{(j)} = \Psi_{N-1}^{(j)} \prod_{j'(\neq j)} \zeta_{N-1}^{(j')}. \tag{A5}$$

The free energy of the Cayley tree is described by the expression

$$-F_N^{Cayley}/T = \ln Z_N = \sum_{j=1}^{q} \ln \zeta_N^{(j)} + \ln \Phi, \qquad (A6)$$

where

$$\Phi = \sum_{\sigma_0} W(\sigma_0) \prod_{j=1}^{q} z^{(j)}(\sigma_0). \qquad (A7)$$

On substituting Eq. (A5) into Eq. (A6) and repeating this recurrent procedure $M$ times, we are led to the following relation for the free energy of the Cayley tree:

$$F_N^{Cayley} = (q-1)^M F_{N-M}^{Cayley} + F_{MN},$$
$$(A8)$$
$$-F_{MN}/T = \sum_{k=1}^{M} (q-1)^{k-1} \sum_{j=1}^{q} \ln \Psi_{N-M}^{(j)}$$
$$- [(q-1)^M - 1] \ln \Phi.$$

The central part of the Cayley tree consisting of $M$ shells can be imaged, at $N \to \infty$, by the Bethe lattice which includes the following number of sites:

$$N_{Site} = \frac{2}{q} N_{Bond} = 2 \frac{(q-1)^M - 1}{q-2}. \qquad (A9)$$

Thus, we arrive at the expression for the free energy of the Bethe lattice per lattice site:

$$-f_{Bethe}/T = \lim_{N \to \infty} (-F_{MN}/N_{Site}T)$$
$$= \frac{1}{2} \sum_{j=1}^{q} \ln \Psi^{(j)} - \frac{q-2}{2} \ln \Phi, \qquad (A10)$$

where $\Psi^{(j)}$ is the limiting value of $\Psi_{N-1}^{(j)}$ at $N \to \infty$. For an isotropic system, the above expression reduces to that reported in Ref. 27.

It is noteworthy that relation (A10) is invariant under the transformation

$$z^{(j)}(\sigma) = \tilde{z}^{(j)}(\sigma) \tilde{\zeta}^{(j)},$$

$$\Psi^{(j)} = \tilde{\Psi}^{(j)} [\tilde{\zeta}^{(j)}]^{-2} \prod_{j'=1}^{q} \tilde{\zeta}^{(j')},$$

$$\Phi = \tilde{\Phi} \prod_{j=1}^{q} \tilde{\zeta}^{(j)}. \qquad (A11)$$

The quantities $\tilde{\zeta}^{(j)}$ can therefore be always chosen so that $\Psi^{(j)} = 1$ for all $j = 1, \ldots, q$. As a result, relation (A10) is expressible in a very simple form convenient for calculations:

$$f_{Bethe} = \frac{q-2}{2} T \ln \tilde{\Phi}, \quad \tilde{\Phi} = \sum_{\sigma_0} W(\sigma_0) \prod_{j=1}^{q} \tilde{z}^{(j)}(\sigma_0),$$
$$(A12)$$

where the quantities $\tilde{z}^{(j)}(\sigma_0)$ satisfy, in terms of relations (A4) and (A11), the system of equations

$$\tilde{z}^{(j)}(\sigma_0) = \sum_{\sigma_1} W_j(\sigma_0, \sigma_1) \prod_{j'(\neq j)} \tilde{z}^{(j)}(\sigma_1). \qquad (A13)$$

Since the second of expressions (A12) and (A13) respectively coincide with Eqs. (A1) and (A2) provided that $\tilde{z}^{(j)}(\sigma_0) = g_N^{(j)}(\sigma_0)$ and $\tilde{\Phi} = Z_N$, one can formally consider Eq. (A2) as a usual system of equations in the variables $g^{(j)}(\sigma_0)$. The quantity $g^{(j)}(\sigma_0)$ thus defined enables calculation of the analog of the partition function $Z$ and the corresponding analog of the free energy. The latter coincides accurate to the factor $(2-q)/2$ with the correct expression for the free energy of the Bethe lattice per lattice site. This technique significantly simplifies the calculations, which is illustrated well by the analysis of the model given in Sec. III.

The efficiency of the above-developed technique is also exemplified by a brief deduction of the free energy for the anisotropic Ising model on the Bethe lattice. The Boltzmann weights $W(\sigma_0)$ and $W_j(\sigma_0, \sigma_1)$ for the anisotropic Ising model with $s = 1/2$ appear as

$$W(\sigma_0) = \exp(h\sigma_0), \quad W_j(\sigma_0, \sigma_1) = \exp(K_j \sigma_0 \sigma_1 + h \sigma_1).$$
$$(A14)$$

Substituting them into the system of equations (A2), we immediately arrive at the solution

$$g^{(j)}(1/2) = \left( \frac{1 - t^2 x_j^{-2}}{1 - t} e^{K_j + h} \tau \right)^{1/2}, \qquad (A15)$$

where

$$\tau \equiv \prod_{j=1}^{q} g^{(j)}(1/2) = \left[ \prod_{j=1}^{q} \left( \frac{1 - t^2 x_j^{-2}}{1 - t} e^{K_j + h} \right)^{1/2} \right]^{2/(2-q)},$$

$$x_j \equiv \frac{g^{(j)}(-1/2)}{g^{(j)}(1/2)}, \quad t \equiv \prod_{j=1}^{q} x_j \qquad (A16)$$

and $x_j$ obeys the equation

$$x_j - t x_j^{-1} = (1-t) e^{-2K_j}. \qquad (A17)$$

The notation specified in Eq. (A16) enables relation (A1) to be written in the form

$$Z = (1+t) e^h \tau, \qquad (A18)$$

which affords, with regard to Eq. (A16), the known expression for the free energy (see Eq. (4.9.6) from Ref. 10):

$$-f_{Behte}/T = h + \frac{1}{2} \sum_{j=1}^{q} K_j + \ln(1+t) + \frac{1}{2} \sum_{j=1}^{q} \ln \frac{1 - t^2 x_j^{-2}}{1 - t^2}. \qquad (A19)$$

*Email address: vrozen@mail.kar.net

[1] C. L. Henley, Phys. Rev. Lett. **62**, 2056 (1989).

[2] J. F. Fernandez, M. Puma, and R. F. Angulo, Phys. Rev. B **44**, 10 057 (1991).

[3] P. I. Belobrov, R. S. Gekht, and V. A. Ignatchenko, Zh. Eksp. Teor. Fiz. **84**, 1097 (1983) [Sov. Phys. JETP **57**, 636 (1983)].

[4] V. M. Rozenbaum and V. M. Ogenko, Fiz. Tverd. Tela (Leningrad) **26**, 1448 (1984) [Sov. Phys. Solid State **26**, 877 (1984)].

[5] S. Prakash and C. L. Henley, Phys. Rev. B **42**, 6574 (1990).

[6] V. M. Rozenbaum, Phys. Rev. B **53**, 6240 (1996).

[7] V. M. Rozenbaum and S. H. Lin, *Spectroscopy and Dynamics of Orientationally Structured Adsorbates* (World Scientific, Singapore, 2002).

[8] J. Ashkin and E. Teller, Phys. Rev. **64**, 178 (1943).

[9] R. V. Ditzian, J. R. Banavar, G. S. Grest, and L. P. Kadanoff, Phys. Rev. B **22**, 2542 (1980).

[10] R. J. Baxter, *Exactly Solved Models in Statistical Mechanics* (Academic Press, London, 1982).

[11] T. Horiguchi and Y. Honda, Prog. Theor. Phys. **93**, 981 (1995).

[12] N. Sh. Izmailian, Pis'ma Zh. Eksp. Teor. Fiz. **63**, 270 (1996) [JETP Lett. **63**, 290 (1996)].

[13] V. M. Rozenbaum and S. H. Lin, J. Chem. Phys. **112**, 9083 (2000).

[14] S. Tang, S. D. Mahanti, and R. K. Kalia, Phys. Rev. B **32**, 3148 (1985).

[15] V. M. Rozenbaum, Pis'ma Zh. Eksp. Teor. Fiz. **63**, 623 (1996) [JETP Lett. **63**, 662 (1996)]; Zh. Eksp. Teor. Fiz. **111**, 669 (1997) [JETP **84**, 368 (1997)].

[16] J. Heidberg, E. Kampshoff, R. Kühnemuth, M. Suhren, and H. Weiss, Surf. Sci. **269/270**, 128 (1992).

[17] V. M. Rozenbaum and A. N. Morozov, Pis'ma Zh. Eksp. Teor. Fiz. **75**, 756 (2002) [JETP Lett. **75**, 631 (2002)].

[18] L. D. Landau and E. M. Lifshitz, *Statistical Physics* (Pergamon Press, New York, 1980).

[19] N. Metropolis, A. W. Rosenbluth, M. N. Rosenbluth, A. H. Teller, and E. Teller, J. Chem. Phys. **21**, 1087 (1953).

[20] S. Romano, Phys. Rev. B **49**, 12 287 (1994).

[21] R. H. Swendsen and J. S. Wang, Phys. Rev. Lett. **58**, 86 (1987).

[22] J. Heidberg, M. Grunwald, M. Hustedt, and F. Traeger, Surf. Sci. **368**, 126 (1996).

[23] P. D. Gujrati, Phys. Rev. Lett. **74**, 809 (1995).

[24] T. P. Eggarter, Phys. Rev. B **9**, 2989 (1974).

[25] E. Müller-Hartmann and J. Zittartz, Phys. Rev. Lett. **33**, 893 (1974).

[26] N. S. Ananikian, A. R. Avakian, and N. Sh. Izmailian, Physica A **172**, 391 (1991).

[27] N. S. Ananikian, N. Sh. Izmailian, and K. A. Oganessyan, Physica A **254**, 207 (1998).